INTERNATIONAL JOURNAL FOR NUMERICAL AND ANALYTICAL METHODS IN GEOMECHANICS, VOL. 21, 599–618 (1997)

ANALYSIS OF SETTLEMENT AND LATERAL DEFORMATION OF SOFT CLAY FOUNDATION BENEATH TWO FULL-SCALE EMBANKMENTS

B. INDRARATNA[1,*,§], A. S. BALASUBRAMANIAM[2,†] AND N. SIVANESWARAN[2,‡]

[1] *Department of Civil and Mining Engineering, University of Wollongong, Wollongong, NSW 2522, Australia*
[2] *Division of Geotechnical Engineering, School of Civil Engineering, Asian Institute of Technology, Bangkok, Thailand*

SUMMARY

In 1986, the Malaysian Highway Authority constructed a series of trial embankments on the Muar Plain (soft marine clay) with the aim of evaluating the effectiveness of various ground improvement techniques. This study investigates the effect of two such ground improvement schemes: (a) preloading of foundation with surface geogrids and synthetic vertical drains and (b) sand compaction piles. The paper is focused on the finite element analysis of settlements and lateral displacements of the soft foundation. In scheme (a), the numerical predictions are compared with the field measurements. In scheme (b), only the numerical analysis is presented and discussed in the absence of reliable measurements due to the malfunctioning of the electronic extensometer and inclinometer system during embankment construction. The current analysis employs critical state soil mechanics, and the deformations are predicted on the basis of the fully coupled (Biot) consolidation model. The vertical drain pattern is converted to equivalent drain walls to enable plane strain modelling, and the geogrids are simulated by linear interface slip elements. The effect of sand compaction piles is investigated considering both ideal drains and non-ideal drains, as well as varying the pile stiffness. © 1997 by John Wiley & Sons, Ltd.

Int. J. Numer. Anal. Meth. Geomech., Vol. 21, 599–618 (1997)
(No. of Figures: 16 No. of Tables: 4 No. of Refs: 22)

Key words: embankments; finite element method; ground improvement; settlements; soft clay; vertical drains

INTRODUCTION

Soft clay foundations in Southeast Asia are mainly of marine, logoonal or deltaic origin. The marine clays in particular are extremely soft and present considerable construction problems. Therefore, the design and construction of surface structures including embankments requires a through geotechnical knowledge of these soft foundations, in order to prevent excessive settlements and associated structural damage. In order to assess the relative performance of different ground improvement methods in soft clay, the Malaysian Highway Authority constructed a series of fifteen trial embankments on the Muar Plain in 1986, as shown in Figure 1. The

* Senior Lecturer
† Chair Professor
‡ Research Associate

§Correspondence to B. Indraratna, Department of Civil and Mining Engineering, University of Wollongong, Wollongong, NSW 2522, Australia.

Contract grant sponsor: Malaysian Highway Authority.

CCC 0363–9061/97/090599–20$17.50

Received 25 October 1995
Revised 31 October 1996

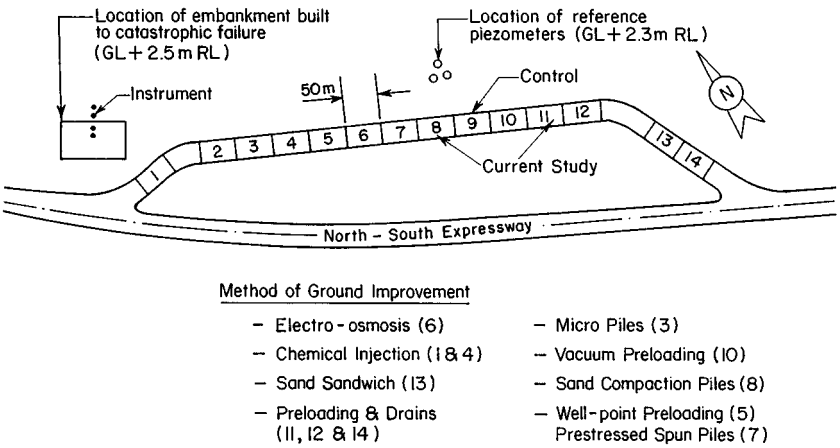

Fig. 1. Relative location of trial embankments along North–South expressway

behaviour of two of these embankments was analysed previously,[1,2] namely, the embankment rapidly constructed to failure on the untreated foundation and the embankment #14 stabilized only with synthetic vertical drains installed in a triangular pattern. This study concentrates on the analysis of the lateral deformation and settlements associated with two different embankments stabilized with (a) preloading, surface geogrids and vertical drains (#11 in Figures 1 and 2) and (b) the other with sand compaction piles (#8 in Figures 1 and 3). The vertical drains of the former and the sand compaction piles of the latter were both installed in a square grid pattern. Studies on the effect of pre-loading with vertical drains have been conducted earlier by Holtz,[3] Nicholson and Jardine,[4] Atkinson and Eldred[5] and Akagi,[6] but their modelling techniques have been different from what is discussed in this paper.

The embankment fill consisted of a granitic residual soil compacted to an average unit weight of 20·5 kN/m^3. While the embankment built above the preloaded foundation with geogrids and vertical drains was raised to a maximum height of 8·7 m, the other constructed over sand compaction piles was raised to a height of 8·8 m, excluding the sand layer above the original ground surface. The rate of construction of the two embankments is shown in Figure 4, where a three-stage linearized sequence was adopted for the numerical analysis. The prefabricated vertical drains and the sand compaction piles were installed to a depth of 20 m in square grid patterns, i.e. 2 m × 2 m and 2·2 m × 2·2 m, respectively. The behaviour of these two embankments was expected to be different from an earlier study,[2] in which synthetic band drains (18 m deep) were installed in a triangular pattern (1·3 m spacing). The previous analysis[2] did not consider any embankment with geogrids.

The prefabricated vertical drains (trade name DESOL) consisted of polyolefine cores, and the sides of these drains were perforated with 0·2 mm diameter holes at 2 mm centres. A total number of 45 band drains were installed, and their equivalent diameter was determined to be 70 mm, based on the cross-section dimensions of the drains. Preloading was carried out by a layer of sand (0·5 m) with 50 mm diameter horizontal drains at 2 m spacing above the ground level. An equal thickness of fill was later removed from the top of the embankment to compensate for this initial surcharge. Two layers of Tensar SR110 geogrids were placed as interface reinforcements between the embankment and the foundation as shown in Figure 2.

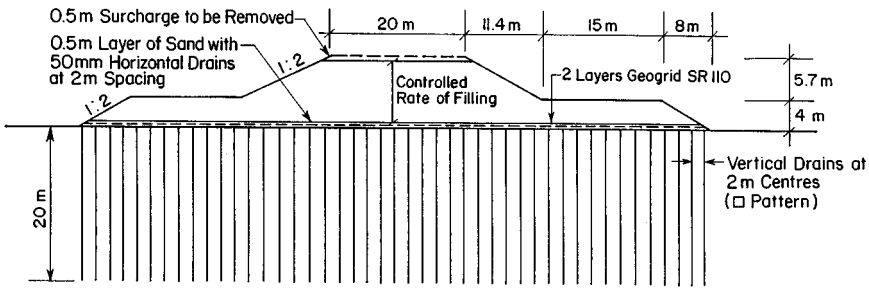

Fig. 2. Embankment constructed on preloaded foundation stabilized with geogrids and vertical drains

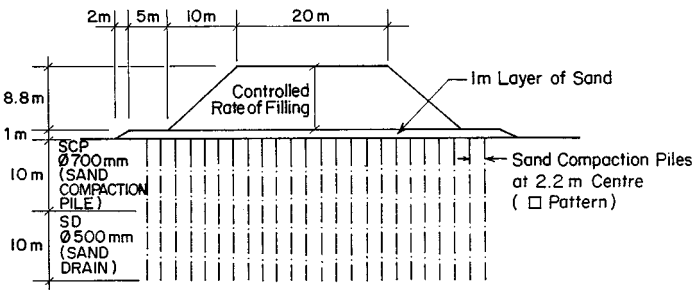

Fig. 3. Embankment constructed on foundation stabilized with sand compaction piles

Sand compaction piles are similar to the mandrel driven sand drains, except that the poured sand is compacted by vibro-flotation. The densified sand columns are expected to have a higher shear resistance than the band drains. Also, the sand compaction piles show less settlement upon surcharge loading (greater stiffness), and they increase the bearing capacity of the foundation more than the conventional sand drains having a smaller compaction density. For this embankment, the compaction of 21 sand columns (700 mm diameter) was carried out only for the top 10 m, while the lower half of the sand columns (500 mm dia) was left uncompacted (i.e. sand drains) as illustrated in Figure 3.

In comparison with the embankment rapidly built to failure on the untreated foundation, excess pore pressure did not develop significantly in the current two cases, because of the relatively dense drain pattern installed in the sub-soil. At depths exceeding 19 m or so, the vertical drains reach the dense sand deposits. The settlements of the foundations were monitored by settlement gauges and extensometers, while the lateral movements were monitored by inclinometers. Surface settlement markers were installed at the top of the completed embankment for monitoring post-construction settlement and heave at the embankment toe. The extensometer systems were installed below the centre line of the embankment and at 23 m away from the centreline, near the vicinity of the toe. All instruments were monitored twice a week during filling and once a week when filling was not taking place. For some embankments, slight variations from the standard instrumentation layout[7] were carried out depending upon the type of ground improvement scheme.

The foundation response is modelled according to the modified cam-clay theory incorporated in the extended finite element code, CRISP, together with a series of additional computer subroutines developed by the authors. The critical state parameters were estimated from undrained k_0-consolidation triaxial tests and consolidation tests. Detailed laboratory procedures are established from which the critical state parameters can be determined.[8] Using the finite element approach adoping the coupled (Biot) consolidation analysis, the time-dependent settlements and lateral yield were predicted. The effect of selected ground improvement schemes on the deformation behaviour of the Muar clay foundation is also highlighted.

SOIL PARAMETERS

The marine clay deposits on the Muar coastal plain have a thickness of up to 20 m with a lateral extent of about 25 km. The uppermost layer of the soil (1·5–2·0 m) is a compacted (weathered) crust with a relatively high pre-consolidation pressure, in comparison with the underlying soft clay (normally consolidated or lightly over-consolidated). The unit weight of Muar clay varies within a small range of 15·5–16 kN/m^3, except at the crust where the unit weight approaches 17·0 kN/m^3. At depths approaching 18 m, a thin organic (peat) layer is sometimes found, followed by a thick dense sand layer. A quantitative description of the geological profile and detailed properties of Muar clay as a function of depth are discussed by Indraratna *et al.*,[1] and given in the Proceedings of International Symposium on Trial Embankments on Malaysian Marine Clays.[7]

In order to estimate the correct soil properties with depth, detailed field and laboratory tests were conducted. These included *in situ* vane and cone penetration tests, a series of triaxial tests based on Consolidated Isotropically Undrained (CIU), k_0-consolidation (CkoU), Consolidated Drained (CD) and constant stress ratio tests. The relationships between the cam-clay parameters and consolidation parameters were also evaluated by oedometer tests. By testing a large number of specimens recovered from different depths, soil parameters corresponding to pre-yield response, the Mohr–Coulomb criterion and the modified cam-clay theory[9] were established.

Deformation analysis based on the modified cam-clay model incorporates the following important parameters, for isotropic compression, swelling and recompression:

λ, κ:	Slope of volume vs. log pressure relationship for consolidation and swelling, respectively,
M:	gradient of the critical state line based on effective stresses,
e_{cs}:	void ratio at unit consolidation pressure,
K, K_w:	bulk moduli of soil and water, respectively,
k_v, k_h:	vertical and horizontal permeability coefficients, respectively,
E_s, G_s, v:	Elastic modulus, shear modulus and Poisson's ratio.

A summary of parameters used in the finite element analysis is given in Table I, where the sub-soil profile is divided into three basic material zones. Cam-clay theory regards λ, κ and M to be unique for a specific yield surface. Nevertheless, the correct values of these parameters are associated with the actual stress path behaviour within a given region of the foundation (Figure 5), where the working stress range must be considered in relation to the pre-consolidation pressure of the sub-soil at a particular depth. The role of the stress paths shown in Figure 5 is to illustrate that from the centreline of the embankment towards the toe of the embankment, the

Table I. Modified cam-clay parameters of Muar clay

Depth (m)	κ	λ^a	e_{cs}	M	υ	$k_w \times 10^{-4}$	γ_s (kN/m^3)	$k_h \times 10^{-9}$ (m/s)	$k_v \times 10^{-9}$ (m/s)
0–2	0·06	0·16	3·10	1·19	0·29	4·4	16·5	6·4	3·0
2–6	0·06	0·16	3·10	1·19	0·31	1·1	15·0	5·2	2·7
6–8	0·05	0·15	3·06	1·12	0·30	2·4	15·5	3·1	1·4
8–18	0·04	0·09	1·61	1·07	0·25	22·7	16·0	1·3	0·6

Note: [a] The values of λ tabulated are for stage 1 loading. At stages 2 and 3 of construction, for depths $> 2{\cdot}0$ m, $\lambda > 0{\cdot}16$. For 2–8 m depth, $\lambda = 0{\cdot}60$ and for 8–18 m depth, $\lambda = 0{\cdot}36$.

accurate values of cam-clay parameters have to be evaluated by appropriate stress paths testing in the laboratory.[8,10] For example, close to the embankment toe where swelling of clay occurs, triaxial extension tests are more realistic than triaxial compression tests.

In the authors' experience, the value of λ is the most influential factor that governs the settlements and lateral deformations. Given the rate of embankment construction (fill thickness) and the corresponding distribution of principal stresses at a given location, the magnitude of λ can either take a smaller value associated with the over-consolidated states (λ_{oc} approaching κ), or at stresses exceeding the pre-consolidation pressure (P_c), it can take the conventional value following the normally consolidated line (λ_{nc}). Considering the plastic volume changes associated with conventional drained behaviour (loading and unloading), the role of the parameters λ_{nc}, λ_{oc} and κ has been explained in detail elsewhere.[10] Given the loading sequence, a value of λ_{oc} equal to 0·16 was used for stage 1, while for greater fill heights (stages 2 and 3), values of λ_{nc} equal to 0·60 (depth: 2–8 m) and 0·36 (depth: 8–18 m) were adopted, as given in Table I.

FINITE ELEMENT ANALYSIS

The purely undrained analysis is useful for predicting the immediate settlements, whereas the coupled (Biot) consolidation model accommodates both the immediate deformation and the consolidation response. Both the undrained and coupled analyses were conducted to compute the immediate and time-dependent deformation. As anticipated, due to the dissipation of excess pore pressures within the foundation via vertical drains or sand compaction piles, the coupled model was considered to be more realistic in representing the actual field conditions in the Muar plain.

Figure 4 illustrates the linearized construction sequence for both embankments, where the rate of loading was simulated by successive addition of elements corresponding to each stage of construction. Each added layer of elements contributes to the increased surcharge load based on the average unit weight. The corresponding body forces due to self-weight is divided into a number of sub-increments, thus representing a separate stage of the numerical analysis. This enabled the computed results of one stage of construction to be incorporated into the next stage (without having to re-run the former), simulating the correct sequential construction procedure described in Figure 4. In the analysis, the potential failure of the embankment itself was not considered, as there was no field evidence to support any form of tensile cracking or shear failure within the compacted fill. A bulk unit weight of 20·5 kN/m^3 and a mean deformation modulus of 5100 kPa were typical of this compacted residual fill, as obtained from *in situ* specimens. The

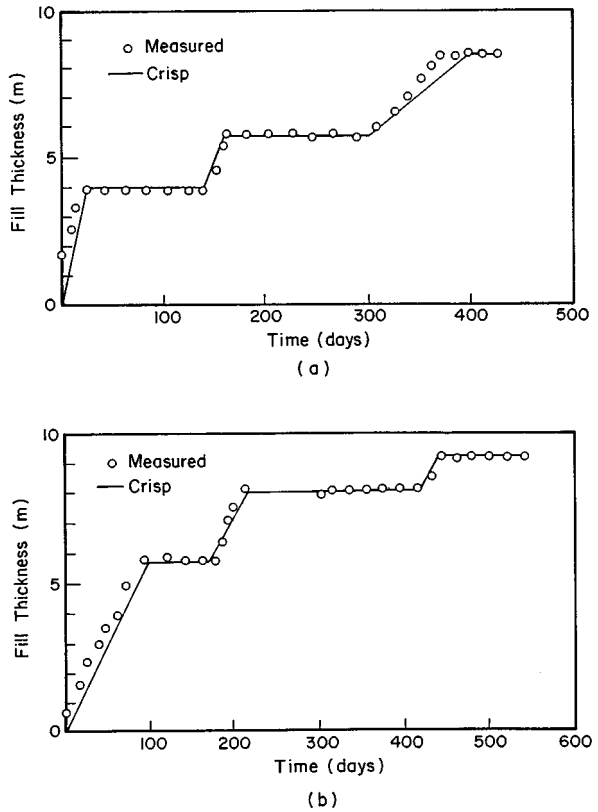

Fig. 4. Idealised construction history of embankments over (a) geogrids and vertical drains and (b) sand compaction piles

enhanced shear strength of the fill (sandy clay) was evident from the consolidated drained triaxial tests which indicated a friction angle of 31° and a cohesion intercept of 15 kPa for laboratory specimens compacted to the same dry density as in the field. The *in situ* stress conditions applied in the finite element analysis are given in Table II, which includes the variation of horizontal and vertical stresses (σ_{x0}, σ_{y0}), groundwater pressure (u) and the isotropic pre-consolidation pressure (P_c) with depth.

In order to compute the settlements and lateral deformation of the soft clay foundation, six layers of Linear Strain Quadrilateral (LSQ) elements were employed in the finite element mesh. The idealized mesh configurations for the two embankments are given in Figures 6 and 7 with the boundary and support conditions. For both cases, it was possible to exploit symmetry and consider one half of the embankment in the analysis, where lateral flow was not permitted across the centre line of the embankments. The maximum horizontal length of the finite element mesh was made at least five times the vertical dimension so that the boundary effect could be minimized. The locations of the horizontal grid lines of the mesh were based on the different material zones identified in Table I. The pattern of vertical grid lines was influenced by the spacing of equivalent drain walls determined for 2-D-plane strain analysis as discussed in detail later.

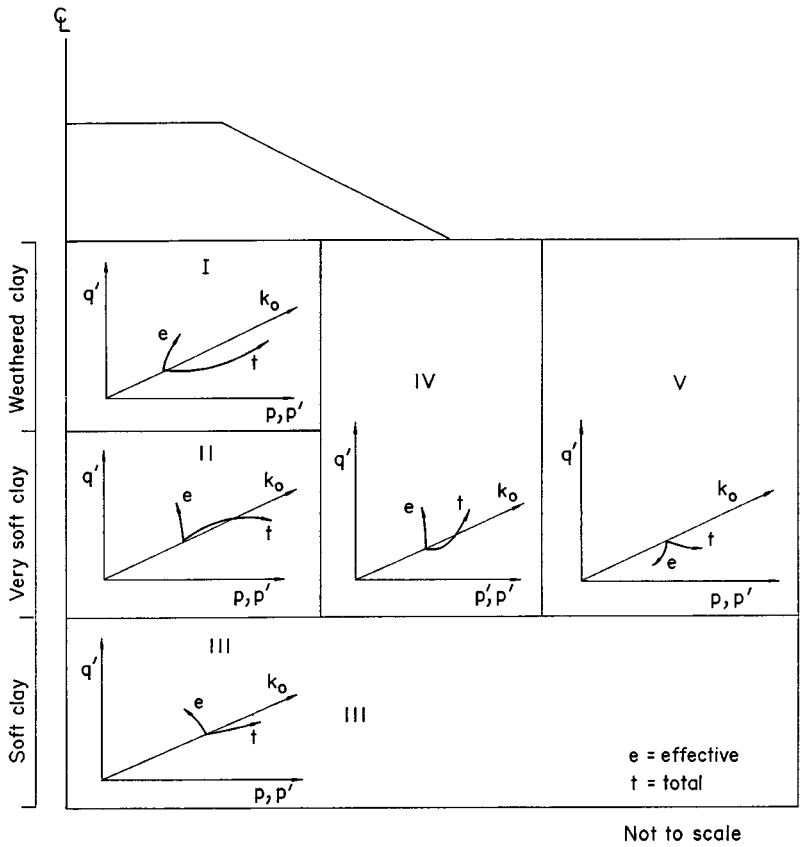

Fig. 5. Nature of stress paths in various locations within the soft clay foundation (Indraratna and Balasubramaniam, 1993)

Table II. In situ stress conditions in the vicinity of Embankments

Depth (m)	σ_{x0}' (kPa)	σ_{y0}' (kPa)	u (kPa)	P_c (kPa)	Soil condition
0	0	0	0	110	Compacted crust
2	19·8	33·0	2·4	90	Very soft clay
6	30·8	51·3	41·6	40	followed by soft
8	37·6	62·6	61·3	60	silty clay
18	74·8	124·6	159·3	> 65	Dense silty clay (relatively stiff)

A rigid foundation depth of 20 m was considered to be sufficient as the dense sand deposit below this depth is much stiffer than the overlying soft clay layers. In fact, the measured field deformations associated with the dense sand are insignificant,[7] thereby justifying the rigid base assumption at a depth of 20 m. The response of the weathered crust (first layer of elements below

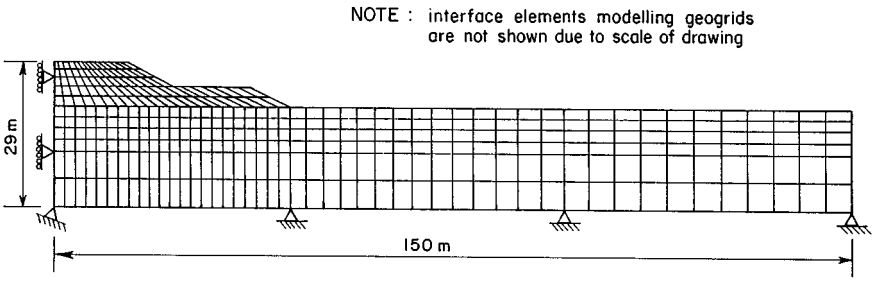

Fig. 6. Finite element mesh for embankment stabilized with geogrids and vertical drains

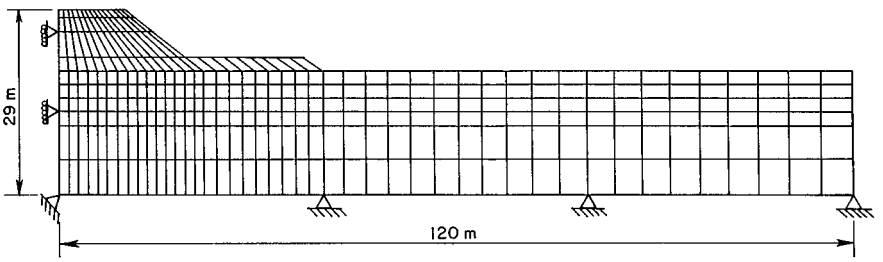

Fig. 7. Finite element mesh for embankment stabilized with sand compaction piles

the ground surface) could be modelled as an overconsolidated material at smaller loads. Limited geological data indicated the possible existence of thin peat partings (100–300 mm) at depths approaching 18 m in the area. Field investigations conducted by the Malaysian Highway Authority indicated that these peat layers were not continuous; their definite occurrence under any particular embankment could not be confirmed. Contributions from many investigators at the International Symposium on Trial Embankments on Malaysian Marine Clays[7] revealed that in any case at such depths, thin peat layers were probably compressed, hence their effect could be ignored. Varying the properties of deep peat partings within acceptable limits has insignificant effect, given the relatively thick soft clay deposits that govern the foundation behaviour. For two other embankments constructed on the same Muar Plain, Indraratna *et al.*[1,2] demonstrated that accurate prediction of foundation settlements and lateral yield could still be made by assuming the same material properties of the overlying soft clay for the thin peat layer located beneath 18 m of soft Muar deposits.

Equivalent drain walls for plane strain modelling

Modelling of the sand compaction piles is similar to that of conventional sand drains, except that the sand compaction piles have a greater stiffness and a higher well resistance. In ideal or perfect drain situations, the effect of well resistance and smear can be neglected. In these two embankments, pre-fabricated band drains and the sand compaction piles were placed in a square grid pattern. The equivalent diameter (d_e) could be determined by $d_e = 1{\cdot}13S$, where S is the spacing of the drains.[11] However, in order to conduct a two-dimensional plain strain analysis, the

vertical drain system was converted to an equivalent drainage wall as illustrated in Figure 8. In principle, L and b_w must satisfy the inequality $B \geqslant 2L + b_w \geqslant S$, where B is the width of the improved zone and S is the actual drain spacing. A modified relationship between the actual vertical drains and the equivalent drainage walls is given below, based on previous work:[12,13]

$$k'_h = k_h \beta (L/d_e)^2; \quad \beta = \frac{2{\cdot}26}{F + \pi G} \tag{1}$$

where d_e is the equivalent diameter of the drain influence zone, L is the half of the distance between two adjacent drain walls, k_h is the natural horizontal permeability of the soil (given in Table I), k'_h is the equivalent horizontal permeability of soil within improved zone, $F = \ln (d_e/d_w) - 0{\cdot}75$, d_w is the actual drain diameter and G is the well resistance factor.

The well resistant factor is related to the coefficient of permeability of the sand walls (k_w), the horizontal permeability of the soil (k_h) and the vertical drainage path length (H). Zeng and Xie[14] have discussed analytical methods of estimating the well-resistant factor, G. The well-resistance delays the consolidation process, if the permeability of the sand columns decreases significantly due to the excessive compaction.

The sand compaction piles were modelled as ideal drains and as non-ideal drains. In the case of ideal drains, the well resistance factor (G) is ignored. If the coefficient of permeability of the sand columns (k_w) is considered to be very large (say > 10 m/s), the value of G becomes negligible, as determined from the following equation:

$$G = (k_h/k_w)\,(H/d_w)^2 \tag{2}$$

The non-ideal drains are characterized by a realistic value of well resistance, $G > 0$. For instance, k_w equals to $1{\cdot}0 \times 10^{-6}$ m/s implies a corresponding value of G of 0·9. The greater the value of G, the lower the rate of consolidation.

The geometrical parameters of the equivalent drain wall model were defined according to two simplified models. For model A, it is assumed that $b_w = 0$ in Figure 8, hence, $L = B/2$, where B is the width of the improved area. An equivalent coefficient of permeability was then assigned to the improved zone by the above theory, with an assumed drainage boundary along the ground surface. For the analysis of prefabricated band drains and geogrids, the ideal drain conditions in Model A were assumed, as the equivalent diameter of band drains (70 mm) was very small compared to the spacing of drains (2·0 m). For model B in which b_w is not negligible, the drain spacing (S) is given by $2L + b_w$. By assuming an equal quantity of sand in the actual and

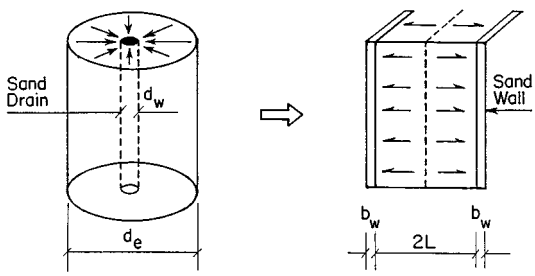

Fig. 8. Conversion of sand drain pattern to a system of sand drain walls

equivalent systems for the same depth of drains, the magnitude of b_w can be determined as:

$$b_w = \frac{\pi d_w^2}{4S} \approx \frac{\pi d_w^2}{8L} \tag{3}$$

Vertical drainage walls were arranged according to their equivalent spacing, and the corresponding equivalent permeability was assigned to the zone stabilized by the drains. Sand compaction piles were analyzed using both Models A and B for ideal and non-ideal drain conditions. In addition, the effect of stiffness of sand compaction piles on vertical and lateral deformations was studied by varying the pile/soil modulus ratio.

Modelling of geogrids

Use of polymeric grids and related products in the stabilization of soft soils and embankments has been discussed by many investigators.[15–18] In high embankments, the geogrids mainly act as reinforcements increasing the soil resistance to deform under load. Their contribution in controlling the settlements and lateral deformation is a function of their stiffness. As shown in Figure 2, the two layers of Tensar geogrids (SR110) were placed at the interface of the embankments base and the sand blanket with the objective of restraining the lateral movements and settlements.

Thin linear interface slip elements (six nodes) were introduced for modelling geogrids, where the deformation mode of these elements was controlled by a normal stiffness, k_n and shear stiffness, k_s, in relation to the applied normal and shear stresses σ_n and τ_s, respectively. The maximum shear stress was defined by the linear Mohr–Coulomb criterion for zero cohesion, where the behaviour was considered elastic if $\tau_s < \sigma_n \tan\phi$. For $\tau_s > \sigma_n \tan\phi$, the analysis permits relative slip between the soil and the structure, but subject to a residual shear stiffness (k_r) which is assumed to be smaller by a factor of 100 than the initial shear modulus (k_s). For the interface, a friction angle (ϕ) of 35°, $k_n = 6870$ kPa, and $k_s = 1962$ kPa were used, based on direct shear tests and pull-out tests conducted on laboratory specimens. Pull out test conditions consider simultaneous shearing on both sides of the geogrid interface. Detailed information on the modelling of such interfaces is given by Desai et al.[19]

Prediction of settlements and lateral deflections

(a) *Foundation with preloading, geogrids and vertical drains.* The settlement profiles along the base of the embankment is illustrated in Figure 9 for all stages of construction. The measured settlements are also plotted for comparison (dashed line). For the same foundation, the calculated settlements (coupled model) are plotted separately for the three idealized cases: (a) preloading with geogrids and drains, (b) preloading with geogrids (no drains) and (c) preloading only, in order to distinguish the different role of the drains and geogrids. However, the overall field conditions are represented by case (a). Ideal drain conditions in Model A were assumed for simulating the behaviour of the pre-fabricated vertical drains. A previous study[20] indicated that the effect of smearing and well resistance of Desol synthetic drains was not significant when installed in soft Muar clay.

As expected, the maximum settlements occur beneath the centre line, and they decrease in magnitude towards the toe of the embankment. Except at stage 1 of loading, the measured

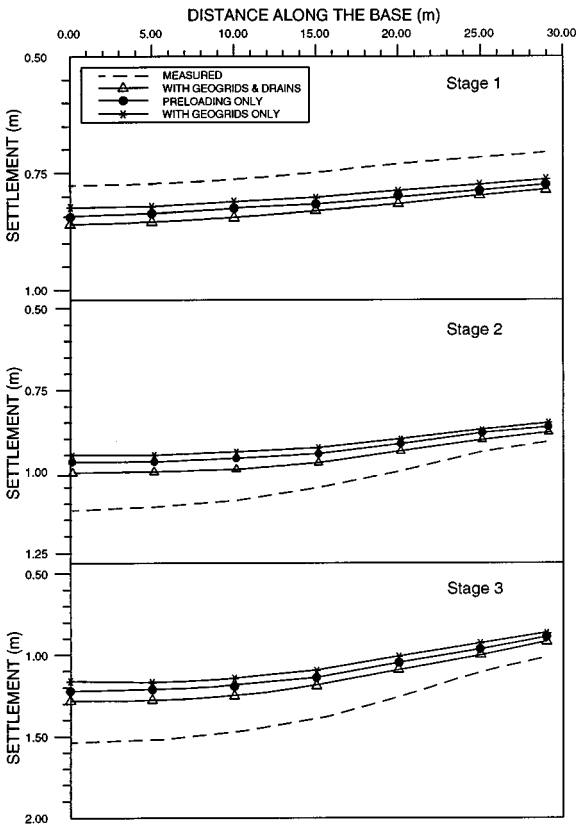

Fig. 9. Predicted and observed settlement profiles for foundation treated with geogrids and vertical drains

settlements are somewhat greater than the predictions, and the deviation from theory is maximum at the centre line. Even though the difference between the three cases of analysis are small, it is evident that the vertical drains increase settlements during the construction of the embankment. Also, the effect of the two layers of Tensar geogrids in resisting settlements is noticeable, although not pronounced. Geogrids having a greater frictional interlock with the surrounding soil should reduce the settlements further. At a distance exceeding 23 m from the centre line of the embankment (i.e. away from the toe, where the foundation is only subjected to berm loading), the foundation settlements with geogrids and drains (case (a)) are closer to the field measurements. In this region, the effects of geogrids and drains diminish as indicated by the convergence of the settlement profiles. It may also be noted that beyond the embankment toe, the sub-soil is free to heave, hence, the resulting net settlements are expected to decrease.

The comparison of predicted and observed settlements with time is shown in Figure 10. The corrected consolidation settlements are derived by subtracting the undrained (immediate) cam-clay predictions from the coupled consolidation model, and subsequently applying the Skempton and Bjerrum settlement coefficient, μ.[21] The settlement of the sub-soil at each stage of construction is also influenced by the enhanced creep at elevated fill heights. The effect of creep on

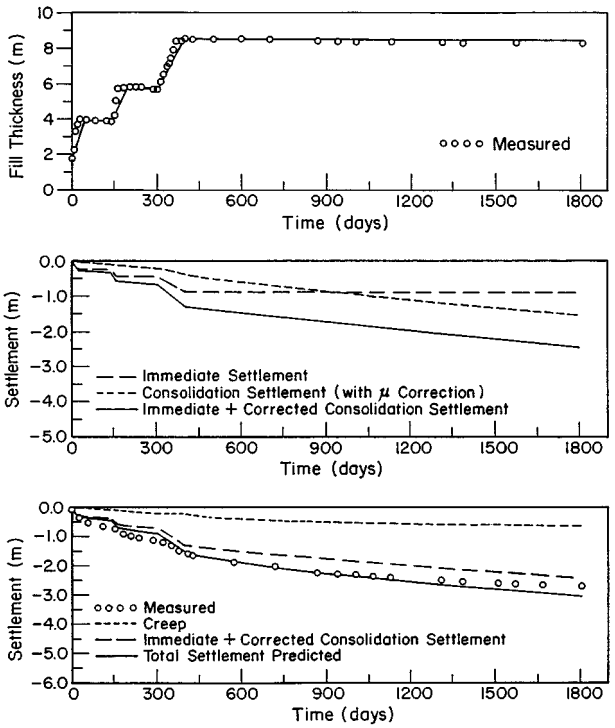

Fig. 10. Comparison of predicted settlements with observations after incorporating creep

settlements could not be directly incorporated into the modified cam-clay model, without significantly changing its conventional volume change vs. shear strain relationships. Consequently, an empirical approach is introduced here, where the creep component as a function of time is estimated using the field deformation analysis (FDA), a methodology established by Loganathan *et al.*[22] for the same Muar clay soils. In FDA, the creep component (ρ_{cr}) and the uncorrected consolidation settlement (ρ_c) are related by the expression: $\rho_c = 29\ \rho_{cr}0{\cdot}5$ (both ρ_c and ρ_{cr} in mm). The predicted total settlement was then obtained by adding the creep component to the combined undrained and corrected consolidation settlement. As illustrated in Figure 10 for the foundation stabilized with geogrids and vertical drains, the measurements and predictions show an excellent agreement after incorporating creep, even four years after the construction of the embankment to its maximum height. The creep component accounts for about 15% of the total settlements after placing the maximum fill at stage 3.

For the same three cases as before, Figure 11 indicates the difficulty in predicting the correct lateral displacements beneath embankment toe, in relation to the measurements. This is mainly attributed to the sensitivity of the lateral deformations to moderate variations in λ. At stage 1, where λ takes a smaller value of 0·16 for the upper layers (weathered crust), the predictions are generally acceptable. However, at larger stress levels (stages 1 and 2), the predicted lateral deflections are a factor of 2–2·5 smaller than the actual measurements. If the normally consolidated value of $\lambda_{nc} = 0{\cdot}60$ is used from the beginning of construction (i.e. including the crust to

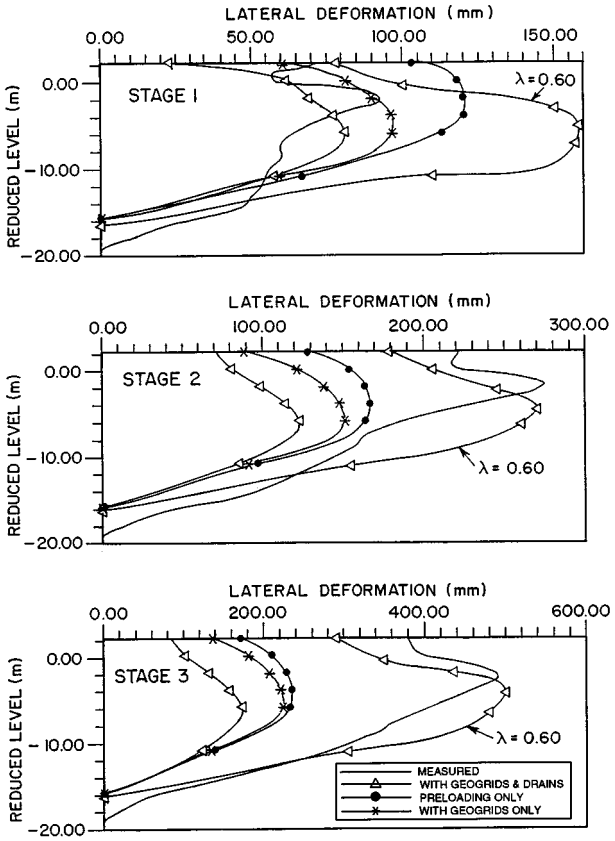

Fig. 11. Predicted and observed lateral displacement profiles for foundation treated with geogrids and vertical drains (beneath the embankment toe)

be a part of the underlying layer), then the stage 1 predictions are significantly over-estimated, but the stage 2 and stage 3 predictions become closer to the measurements (Figure 11). This signifies that the effect of crusting is predominant at low stress levels.

The predicted curves clearly reveal that the geogrids are effective in curtailing the lateral displacements. The effect on lateral displacements is also governed by the residual shear stiffness (k_r) of the interface elements used in the analysis, which was assumed to be a factor of 100 less than the initial shear stiffness. In general, the prediction of settlements from the coupled consolidation model is more reliable in comparison with the lateral displacement predictions. This is because the settlements are not as sensitive as lateral displacements to moderate changes in λ and k_r. As mentioned earlier the accurate prediction of lateral deformations requires the proper evaluation of cam-clay parameters associated with the correct stress paths at different zones in the foundation (Figure 5).

The effect of geogrids on the development of shear stresses beneath the embankment toe (23 m from the centre line) is illustrated in Figure 12 for two identical embankments with and without geogrid reinforcements. It is shown that as the surcharge load is increased, the effect of geogrids

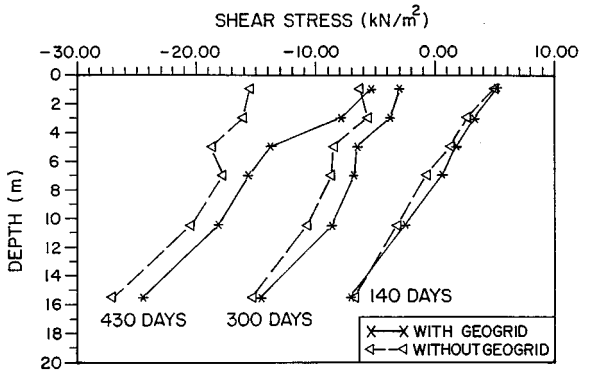

Fig. 12. Effect of geogrids on shear stress distribution 22·5 m away from centreline

Table III. Parameters of equivalent sand drain walls for 2D-plane strain analysis

	Model	b_w (mm)	L (m)	β	k_w (m/s)	k'_h/k_h
Ideal drains	A	0	22·0	4·35	10	339·6
($G = O$)	B	175	1·01	4·35	10	0·72
Non-ideal drains	A	0	22·0	0·68	10^{-6}	53·1
($G = 0·9$)	B	175	1·01	0·68	10^{-6}	0·11
Original sand drain system: $d_w = 700$ mm, $S = 2·2$ m, $d_e = 2·49$ m						

on the reduction of disturbing shear stresses is significant. The reduction in shear stresses is associated with the decreases in lateral movement as shown earlier in Figure 11. Particularly at stage 3, the pronounced influence of the geogrids is illustrated by a marked reduction in shear stresses close to the ground surface. As expected, the effect of geogrids decreases with increasing depth.

(b) *Behaviour of foundation with sand compaction piles.* The effect of sand compaction piles was studied considering both ideal drains and non-ideal drains with well-resistance, assuming the same bulk deformation modulus (K) for the sand piles and the surrounding soil. Both geometric models A and B were considered in the analysis, and the equivalent drain parameters are given in Table III. The settlement profiles along the embankment base are shown in Figure 13, where Model A ($b_w = 0$ in Figure 8) gives greater settlements than Model B, based on the coupled consolidation model. For both Models A and B, the non-ideal drains ($G = 0·9$) are associated with slightly smaller settlements than the ideal drains ($G = 0$), verifying that increasing the well-resistance delays the consolidation process. It is also of interest to note that the well-resistance is more significant in Model A. The field measurements are not plotted because the sondex extensometer and inclinometer systems ceased to function during stage 1, and even the few available readings were considered to be unreliable.

The predicted lateral displacements beneath the toe of the embankment are shown in Figure 14, where the Model A predictions (approaching 280 mm at stage 3) are significantly greater than

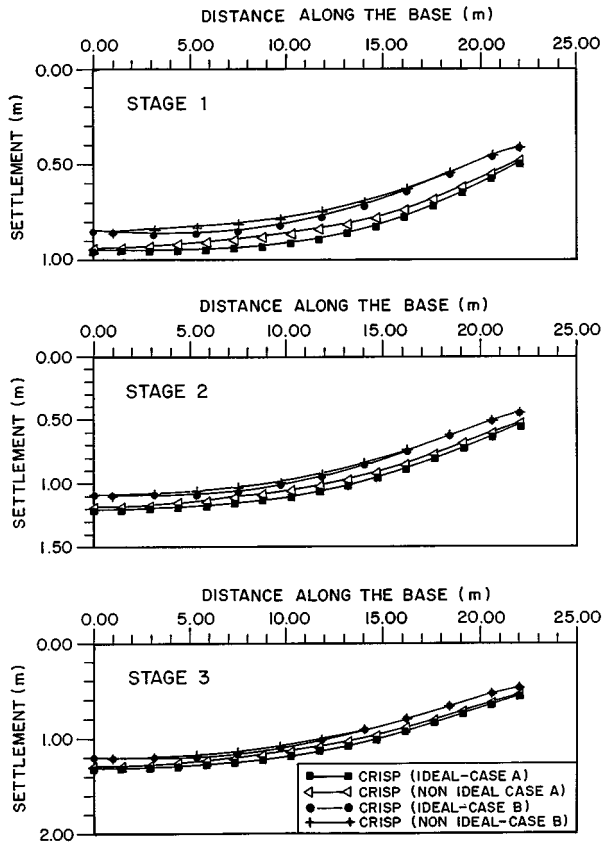

Fig. 13. Predicted settlement profiles for foundation stabilized with sand compaction piles for various stages of embankment construction

those of Model B (less than 220 mm). As the difference between the ideal and non-ideal models is small, the well resistance does not seem to influence the lateral movements to any significant extent. The results shown in Figure 14 are based on the assumption that the stiffness of the sand columns and the surrounding soil is the same. Therefore, not surprisingly, these lateral deflections are significantly higher than those corresponding to the geogrids and drains (Figure 11). In reality, the deformation modulus of a sand compaction pile is several times greater than the soft foundation soil. In order to study the effect of stiffness of sand compaction piles, the pile/soil modulus ratio (K_p/K_s) was increased from 1 to 10. The resulting settlements and lateral displacements ($\lambda = 0{\cdot}16$ for the upper strata) are shown in Figure 15 and 16, respectively. Considering the 700 mm diameter sand piles, Model B was considered to be more appropriate. As expected, with the increase in pile stiffness, both the vertical and lateral displacements decrease significantly. However, the increase in pile stiffness does not affect the location of the maximum lateral movements which occurs at a depth of about 4–5 m RL.

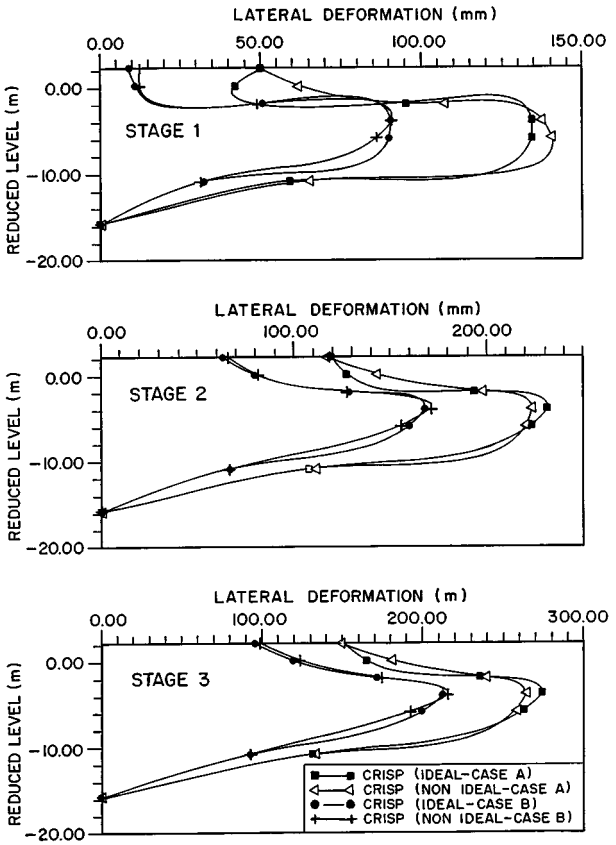

Fig. 14. Predicted lateral displacement profiles for foundation stabilized with sand compaction piles

COMPARISON OF NORMALISED DEFORMATIONS

In order to interpret the deformation analysis further, the following normalized parameters are introduced:

α = ratio of maximum lateral displacement at the toe to the maximum settlement at centre line (α also equals to β_1/β_2)
β_1 = ratio of maximum lateral displacement to the corresponding fill height
β_2 = ratio of maximum settlement to the corresponding fill height

Table IV gives the above normalized deformation factors evaluated for several embankments at their maximum fill heights including the current study. For the sand compaction piles, a pile/soil stiffness ratio of five is assumed. The effect of the surface crust (over-consolidated) is modelled with $\lambda = 0{\cdot}16$. In comparison with the embankment constructed to failure,[1] the stabilized foundations are characterized by considerably smaller values for α and β_1, highlighting their obvious implications on stability. The normalized settlement (β_2) on its own does not seem to be a proper indicator of instability. Nevertheless, the significantly reduced normalized

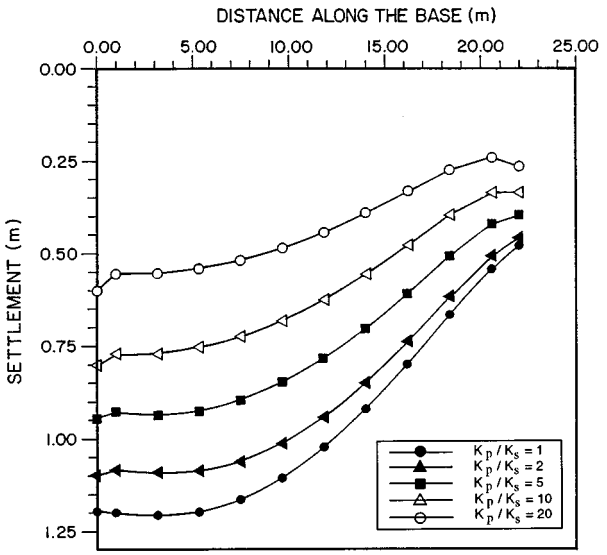

Fig. 15. Effect in increasing pile/soil stiffness ratio on settlement

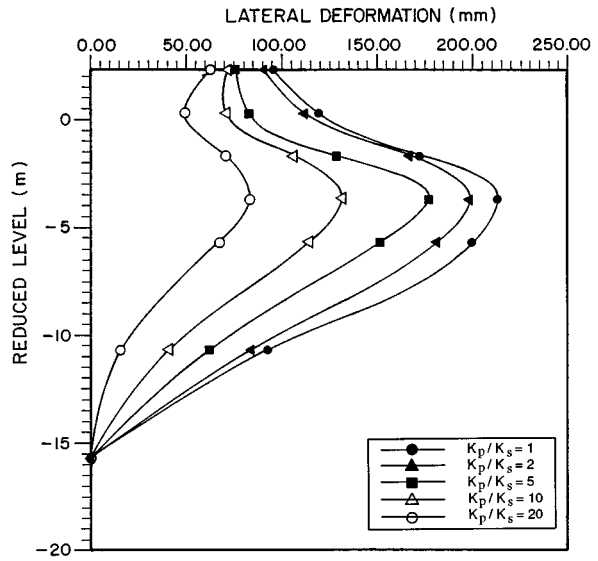

Fig. 16. Effect of increasing pile/soil stiffness ratio on lateral deformation

settlements (β_2) of the sand compaction piles is clearly a function of the prescribed relative pile stiffness. The foundation stabilized only with vertical drains[2] gives the highest values of β_1 and β_2, clearly suggesting the benefits of sand compaction piles and geogrids. Nevertheless, its deformation factor α is the smallest, implying that this embankment could have been raised further than just 4·75 m.

Table IV. Effect of ground improvement on normalized deformation factors

Ground improvement scheme	α	β_1	β_2
Sand compaction piles for pile/soil stiffness ratio of 5 ($h = 9{\cdot}8$ m, including 1 m sand layer)*	0·185	0·018	0·097
Geogrids + vertical band drains in square pattern at 2·0 m spacing ($h = 8{\cdot}7$)*	0·141	0·021	0·149
Vertical band drains in triangular pattern at 1·3 m spacing[a] ($h = 4{\cdot}75$ m)	0·123	0·034	0·274
Embankment rapidly constructed to failure on untreated foundation[b] ($h = 5{\cdot}5$ m)	0·634	0·104	0·164

Note: * Current study; [a,b] references; h = maximum surcharge height

CONCLUSION

Two trial embankments one with geogrids and vertical drains, and the other with sand compaction piles were analysed in detail using the modified cam-clay theory incorporated in the finite element method. In the former, the predictions were compared with the actual field measurements. The following conclusions are drawn on the basis of this study.

The settlements of the stabilized clay foundations subject to embankment loading can be predicted reliably by the coupled consolidation model. However, the accurate prediction of lateral displacements depends on the correct assessment of the value of λ, the shear resistance at the embankment–foundation interface, and the nature of assumptions made in the modelling of drains and sand piles. The actual soil properties are influenced by the working stress range and the assumed stress path of the sub-soil at a given depth. The normally consolidated parameters associated with the cam-clay theories over-estimate lateral displacements and settlements, if the applied stresses are smaller than the pre-consolidation pressure. Usually, greater accuracy is obtained at higher stages of construction.

The analysis of foundation with geogrids and vertical drains verified that creep deformation under relatively high embankment loads must be incorporated to accurately predict the total settlements. The creep component was up to 15% of the total settlements after stage 3 loading (i.e. fill height exceeding 8 m). This study has shown that the use of geogrid reinforcements at the base of the embankment decreases the shear stresses, hence the lateral deformations, particularly close to the ground surface. Therefore, geogrids enable the construction of higher embankments, offering an alternative for the use of additives in surface stabilization to create a stiffer base.

The finite element analysis of sand compaction piles indicated that while the well resistance has little effect on foundation deformation, increasing the ratio of pile to soil stiffness causes the settlements and lateral displacements to decrease substantially. If the modulus of sand compaction piles is assumed to be the same as that of the surrounding soil, then the resulting lateral displacements are significantly greater than those corresponding to the geogrids plus drains combination. The use of a two-dimensional plane strain model in the analysis of these two embankments could be justified by converting the three-dimensional vertical drains to an equivalent two-dimensional drain wall system by assigning an equivalent coefficient of permeability within the improved zone. Although quicker and convenient, the authors do not propose that

plane strain analysis is more superior to a three-dimensional analysis, where radial flow to each drain can be modelled in an explicit manner.

Considering the overall behaviour of both these embankments in comparison with the embankment constructed to failure on untreated clay,[1] the benefits of installing sand compaction piles, geogrids and vertical pre-fabricated drains are obvious. The final heights of the two embankments (8·7 m and 8·8 m) analysed in this study are much greater than the critical height of the failed embankment (5·5 m), and also, the ratios of maximum lateral deformation to maximum settlement are considerably smaller than those of the untreated foundation. This signifies the enhanced stability attributed to these two ground improvement schemes, even though direct comparisons are somewhat questionable because of the different construction rates.

ACKNOWLEDGEMENTS

The continuing support of the Malaysian Highway Authority is appreciated. On various occasions, useful discussions and comments made by Siew-Ann Tan (National University of Singapore), Dr. A. Britto (Cambridge University) and Dr. E.W. Brand (Geotechnical Control Office, Hong Kong) are acknowledged.

REFERENCES

1. B. Indraratna, A. S. Balasubramaniam and S. Balachandran, 'Performance of test embankment constructed to failure on soft marine clay', *J. Geotech. Eng.*, ASCE, **118,** 12–33 (1992)
2. B. Indraratna, A. S. Balasubramaniam and P. Ratnayake, 'Performance of embankment stabilised with vertical drains on soft clay', *J. Geotech. Eng.*, ASCE, **120,** 257–273 (1994).
3. R. D. Holtz, 'Preloading with prefabricated vertical strip drains', *Proc. Seminar on Very Soft Soil Stabilization using High Strength Geosynthetics*, Geosynthetic Research Institute, Drexel University, Philadelphia, 1987, pp. 104–129.
4. D. P. Nicholson and R. J. Jardine, 'Performance of vertical drains at Queensborough Bypass', *Geotechnique*, **31,** 67–90 (1981).
5. M. S. Atkinson and P. J. L. Eldred, 'Consolidation of soft soils using vertical drains', *Geotechnique*, **31,** 33–43 (1981).
6. T. Akagi, 'Effects of mandrel driven sand drains on soft clay', *Proc. 10th Int. Conf. Soil Mech. Found. Eng., Vol.* 3, ISSMFE, Stockholm, 1981, pp. 581–584.
7. *Proc. Int. Symp. on Trial Embankments on Malaysian Marine Clays, Vols.* 1 *and* 2, Malaysian Highway Authority, Kuala Lumpur, Malaysia, 1989.
8. A. M. Britto and M. J. Gunn, *Critical State Soil Mechanics via Finite Elements*, Ellis Horwood, Chichester, U.K., 1987.
9. K. H. Roscoe and J. B. Burland, 'On the generalized stress strain behaviour of wet clay', in *Engineering Plasticity*, Cambridge University Press, Cambridge, U.K., 1968.
10. B. Indraratna and A. S. Balasubramaniam, Author's Closure: 'Performance of test embankment constructed to failure on soft clay', *J. Geotech. Eng., ASCE*, **119,** 1321–1329 (1993).
11. S. Hansbo, 'Consolidation of fine grained soils by prefabricated drains', *Proc. 10th Int. Conf. Soil Mech. Found. Eng., Vol.* 3, ISSMFE, Stockholm, 1981, pp. 677–682.
12. C. C. Hird, I. C. Pyrah and D. Russell, 'Finite element modelling of vertical drains beneath embankments on soft ground', *Geotechnique*, 42, 499–511 (1992).
13. Y. K. Cheung, P. K. K. Lee and K. H. Xie, 'Some remarks on two and three dimensional consolidation analysis of sand-drained ground', *Comp. Geotechnics*, **12,** 73–87 (1991).
14. G. X. Zeng and K. H. Xie, 'New development of vertical drain theories', *Proc. 12th Int. Conf. on Soil Mech. Found. Engng.,* ISSMFE, Rio de Janeiro, Brazil 1989, pp. 1435–1438.
15. R. K. Rowe and K. L. Soderman, 'Stabilization of very soft soils using high strength geosynthetics: the role of finite element analysis', *Geotextiles Geomembranes*, **6,** 53–80 (1987).
16. R. A. Jewell, 'Application of revised design charts for steep reinforced slopes', *Geotextiles Geomembranes*, **10,** 203–233 (1991).

17. R. M. Koerner, *Designing with geosynthetics*, 3rd edn, Prentice-Hall, Englewood Cliffs NJ, 1994.
18. M. R. Hausmann, *Engineering Principles of Ground Modification*, McGraw-Hill, New York, 1990.
19. C. S. Desai, M. M. Zaman, J. G. Lightner and H. J. Siriwardena, 'Thin layer element for interfaces and joints', *Int. j. numer. anal. methods geomech.*, **8,** 19–43 (1984).
20. P. Ratnayake, 'Performance of test embankments with and without vertical drains at Muar Flats, Malaysia', *M. Eng thesis*, Asian Institute of Technology, Bangkok, Thailand, 1993.
21. A. W. Skempton and L. Bjerrum, 'A, contribution to settlement analysis of foundations on clay', Geotechnique, **7,** 168–178 (1957).
22. N. Loganathan, A. S. Balasubramaniam and D. T. Bergado, 'Deformation analysis of embankments', J. Geotech. Eng. ASCE, **119,** 1185–1206 (1993).

